Supporting Information

Zhu et al. 10.1073/pnas.0914231107

SI Materials and Methods

Plasmid and Reagents. For bacterial expression, $SidM_{193–550}$ and $SidM_{317–647}$ were cloned into the pGEX-6p-2 vector (GE Healthcare). The point mutants of SidM used for the GDF and GEF assays were constructed on the $SidM_{193–550}$ background in the pGEX-6p-2 vector. Full-length Rab1a and Rab1a (residues 1–177) were cloned into pET28a (Novagen). Human GDI2 also was cloned into pGEX-6p-2, and a 3×Flag tag was introduced to its N terminus using a PCR-based strategy. Yeast expression plasmids for Rab1 and GDI2 were constructed by inserting PCR fragments of His-Rab1a and GST–3×Flag-GDI2 into the pYES2 and pYES3 vectors (Invitrogen), respectively. Truncation mutants and all point mutation constructs were constructed by standard PCR cloning strategies. All plasmids were verified by DNA sequencing. The Rab1 and GST antibodies were purchased from Santa Cruz Biotechnology. The GDI2 antibody was obtained from Proteintech Group. Mant-GppNHp and mant-GDP were obtained from Jena Bioscience. All other chemicals were Sigma-Aldrich products unless noted otherwise.

Expression and Purification of Recombinant Proteins. GST-SidM proteins were expressed in B834(DE3) strain (Novagen) at 22 °C with 12 h of IPTG induction (0.4 mM). Native proteins and selenomethionine (SeMet) derivatives used for crystallization were expressed in LB and M9 medium, respectively. GST fusion proteins were affinity-purified using glutathione-Sepharose resin (GE Healthcare), and the GST tag was removed by homemade PreScission protease digestion. GST-SidM was further purified on a Sephadex 75 gel-filtration column (GE Healthcare). Native His-Rab1 was expressed in the BL21(DE3) strain. The SeMet derivative of His-Rab1 was expressed in the B834(DE3) strain. His-Rab1 (both full-length and residues 1–177) was purified using Ni-NTA resin (Qiagen), followed by sequential HiTrap Q HP ion exchange (GE Healthcare) and Sephadex 75 gel-filtration chromatography. To prepare the SidM-Rab1 complex, purified $SidM_{193–550}$ was incubated with His-Rab1 (residues 1–177) at a molar ratio of 1:2 at room temperature for 2 h in buffer containing 50 mM Tris-HCl (pH 7.5), 150 mM NaCl, and 10 mM EDTA. The stable complex was obtained after Sephadex 75 gel-filtration chromatography (to remove unbound Rab1 and released nucleotides). All purification processes were performed at 4 °C unless noted otherwise.

Yeast expression of Rab1-GDI complex was performed as described previously (1). In brief, pYES2-His-Rab1 and pYES3-GST–3×Flag-GDI plasmid were cotransformed into FY834, and the transformed yeast cells were grown at 30 °C in the standard minimal SD medium. Cells were transferred to 2% galactose-containing SD medium at OD_{600} 1.0 to induce protein expression. Then 16 h later, cells were lysed by French press in buffer containing 50 mM Tris-HCl (pH 7.5), 150 mM NaCl, 2 mM $MgCl_2$, and 1 mM β-mercaptoethanol. Centrifugated lysates were loaded on the Ni-NTA resin and then eluted with 300 mM imidazole. The stable Rab1-GDI complex was obtained after further purification on the glutathione-Sepharose resin and subsequent removal of the GST tag.

Crystallization and Data Collection. Native and SeMet derivatives of $SidM_{317–647}$ or the $SidM_{193–550}$–Rab1 complex were concentrated in buffer containing 50 mM Tris-HCl (pH 7.5) and 150 mM NaCl to 10 mg/mL and 15 mg/mL, respectively. Native proteins were used for initial crystal screening, and crystal optimization and data collection were performed with SeMet derivatives. SeMet $SidM_{317–647}$ was mixed with 4 mM Tris-(2-carboxyethyl)phosphine before crystallization. Microseeding was used to optimize the diffraction of SeMet $SidM_{317–647}$ crystals, which were finally obtained in 0.6 M potassium sodium tartrate, 0.1 M 2-(N-cyclohexylamino)ethane sulfonic acid (CHES) (pH 9.0), 0.1 M Li_2SO_4, and 0.1 M sodium acetate at 20 °C. Crystals of SeMet $SidM_{193–550}$–Rab1 complex were obtained in 7 days in 1.1 M ammonium sulfate, 0.1 M sodium citrate (pH 5.6), 0.4 M Li_2SO_4, and 0.1 M di-ammonium tartrate at 4 °C. All crystallization experiments were carried out with the hanging-drop vapor diffusion method. Before mounting, crystals of SeMet $SidM_{317–647}$ were soaked in buffer containing 5.6 M sodium formate, 0.1 M CHES (pH 9.0), and 10% reservoir buffer for about 3 min. Crystals of SeMet $SidM_{193–550}$–Rab1 complex were transferred into the well solution supplemented with 15% glycerol as the cryoprotectant, and then flash-cooled in liquid nitrogen. The anomalous diffraction data (Se-Peak) of $SidM_{317–647}$ and the $SidM_{193–550}$–Rab1 complex were collected on BL-5A and NW-12A beamlines at the KEK photon factory (Tsukuba, Japan). All diffraction data were processed using the HKL-2000 package (HKL Research, Inc.).

Structural Determination and Refinement. Crystallographic phases were obtained by Se-SAD using the Phenix program (2). For the complex structure, two copies of $SidM_{193–550}$–Rab1 heterodimers were found in an asymmetric unit. Automatic model building in Phenix provided a 50%-complete model, and the remaining residues were built manually in Coot (3). The structure was refined to 2.85 Å in Refmac5 (4). As for the Rab1-free structure, two $SidM_{317–647}$ molecules in an asymmetric unit were related by noncrystallographic symmetry (NCS). A total of 22 Se atoms in one asymmetric unit were located during the phasing process. The entire main chain was then modeled confidently, occasionally guided by the high-resolution structure of $SidM_{193–550}$. The structure was refined in CNS1.2 (5) using NCS_restrain and group B refinements. Electron densities of the side chains were improved by B-sharpening with a B-factor value of −120 $Å^2$, after which most of the side chains could be easily modeled. The structure of $SidM_{317–647}$ was finally refined to 3.45 Å, with an R_{work}/R_{free} value of 21.45%/24.05% and a high-quality structural geometry. Both models were checked with PROCHECK software (6). Statistics on data collection and refinement are given in Table S1. All structural pictures were drawn in PyMOL (http://www.pymol.org/).

Pulldown and Lipid-Binding Overlay Assays. Purified GST-ubiquitin or GST–$SidM_{193–550}$ was immobilized onto glutathione Sepharose resin, after which the beads were incubated with bacterially purified full-length Rab1 or GDI2 in buffer containing 50 mM Tris-HCl (pH 7.5), 150 mM NaCl, and 1% Nonidet P-40 at 4 °C for 2 h. The beads were extensively washed with the binding buffer and analyzed by Coomassie blue staining on a SDS/PAGE gel. The PtdIns(4)P binding of WT and mutant $SidM_{317–647}$ proteins was performed using the protein-lipid overlay assay as described previously (7). Each binding assay used 200 nM of indicated GST fusion proteins. The binding of GST fusion proteins to lipids immobilized on the nitrocellulose membrane (PIP Strips; Echelon Biosciences) was analyzed by Western blot using an anti-GST antibody.

GDF and GEF Assays. For the GDI displacement assay, 1 μg of Rab1-GDI2 complex immobilized onto Flag M2 beads was incubated with 5 μg of purified $SidM_{193–550}$ for 60 min at room temperature in 40 μL of reaction buffer containing 50 mM Tris-HCl (pH 7.5), 150 mM NaCl, and 2 mM $MgCl_2$. The released Rab1 proteins in su-

pernatant and GDI proteins on beads were detected by Western blot analysis using antibodies for Rab1 and GDI2, respectively.

For the GTP-incorporation assay of SidM GEF activity, nucleotide-free Rab1 was loaded with GDP by 2 h of incubation in the GDP-loading buffer [50 mM Tris-HCl (pH 7.5), 150 mM NaCl, 5 mM EDTA, and 1 mM DTT]. GDP binding was stabilized by adding 10 mM of $MgCl_2$. Free GDP was removed by gel-filtration chromatography. Rab1-GDP (2 μM) was incubated with 0.2 μM of SidM proteins in the presence of 10 μM of fluorescent GTP analog mant-GppNHp in the reaction buffer [50 mM Tris-HCl (pH 7.5), 150 mM NaCl, and 2 mM $MgCl_2$]. Samples were excited at 360 nM, and the emissions resulting from binding of mant-GppNHp to Rab1 were monitored at 460 nM with a GENios Plus microplate fluorescence reader (Tecan). To measure GDP release, nucleotide-free Rab1 was similarly loaded with mant-GDP, and 10 μM of GTPγS was added into each reaction. GDP release was determined by measuring the decrease of the fluorescence resulting from dissociation of mant-GDP from Rab1.

An ^{35}S-labeled GTPγS–uptake assay of the Rab1-GDI complex was performed as described previously (1). Here 15 pmol of WT or the quadruple mutant Rab1-GDI complex was incubated in reaction buffer containing 50 mM Tris-HCl (pH 7.5), 150 mM NaCl, and 5 mM $MgCl_2$ supplemented with 2 pmol of ^{35}S-GTPγS (PerkinElmer) and 30 pmol of unlabeled GTPγS at room temperature. The nucleotide-exchange reaction was initiated by adding 10 pmol of $SidM_{193–550}$, and samples were analyzed by scintillation counting at the indicated time points.

1. Machner MP, Isberg RR (2007) A bifunctional bacterial protein links GDI displacement to Rab1 activation. *Science* 318:974–977.
2. Adams PD, et al. (2002) PHENIX: Building new software for automated crystallographic structure determination. *Acta Crystallogr D Biol Crystallogr* 58:1948–1954.
3. Emsley P, Cowtan K (2004) Coot: Model-building tools for molecular graphics. *Acta Crystallogr D Biol Crystallogr* 60:2126–2132.
4. Collaborative Computational Project Number 4 (1994) The CCP4 suite: Programs for protein crystallography. *Acta Crystallogr D Biol Crystallogr* 50:760–763.
5. Brünger AT, et al. (1998) Crystallography & NMR system: A new software suite for macromolecular structure determination. *Acta Crystallogr D Biol Crystallogr* 54: 905–921.
6. Laskowski AR, MacArthur WM, Moss SD, Thornton MJ (1993) PROCHECK: A program to check the stereochemical quality of protein structures. *J Appl Cryst* 26:283–291.
7. Brombacher E, et al. (2009) Rab1 guanine nucleotide exchange factor SidM is a major phosphatidylinositol 4-phosphate–binding effector protein of *Legionella pneumophila*. *J Biol Chem* 284:4846–4856.

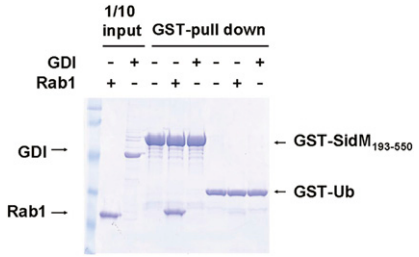

Fig. S1. In vitro binding assay of SidM with Rab1 and GDI. Purified GST–$SidM_{193–550}$ immobilized onto glutathione-Sepharose resin was incubated with bacterially purified full-length Rab1 or GDI2. The beads were extensively washed with the binding buffer and analyzed by Coomassie blue staining on a SDS/PAGE gel. GST-ubiquitin was used as the control.

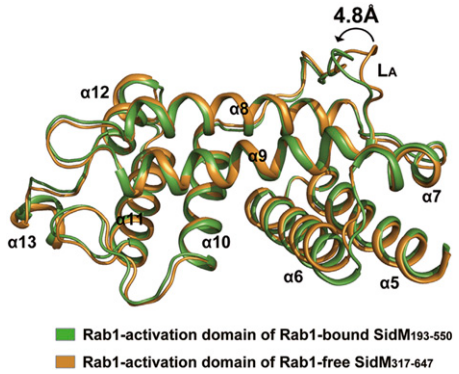

Fig. S2. Superimposition of Rab1-activation domains of $SidM_{317–647}$ alone (yellow) and $SidM_{193–550}$ from the SidM-Rab1 complex (green). The secondary structures are denoted by numbered labels. The two structures are well superimposed except for the long loop L_A, which moves toward α8 and α9 in the Rab1-bound structure by 4.8 Å.

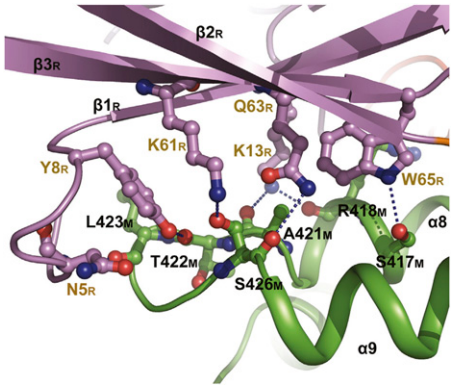

Fig. S3. Interaction of SidM with the N terminus and interswitch of Rab1. Rab1 and SidM are shown in purple and green, respectively. The interacting residues, shown as ball-and-stick representations, are denoted by orange (Rab1) and black (SidM) labels. The secondary structures of SidM and Rab1 involved in the interaction are labeled as well.

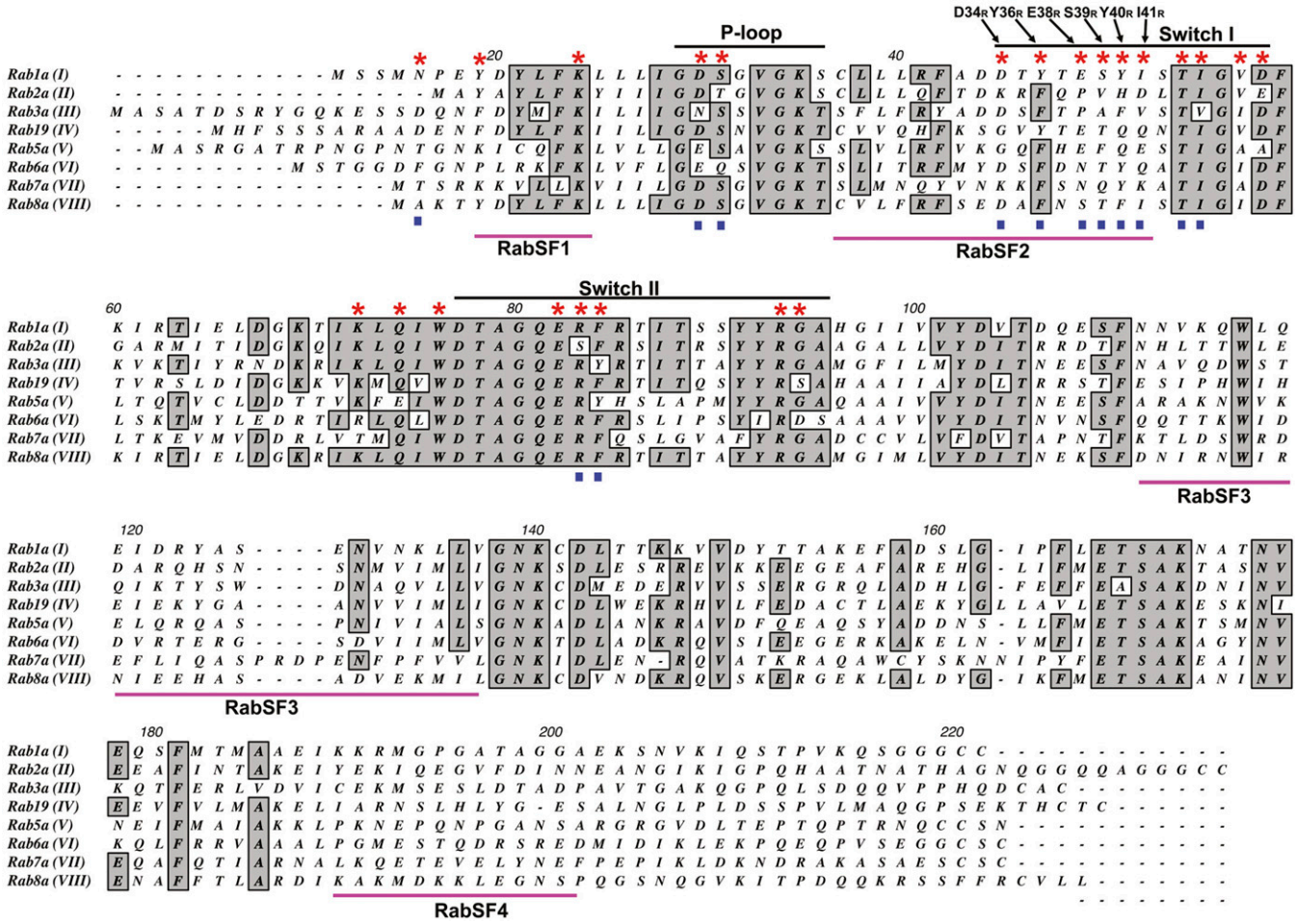

Fig. S4. Multiple sequence alignment of the Rab family. The representative Rab proteins shown in the alignment were selected from the eight Rab subfamilies (I–VIII) and aligned using MacVector software. The conserved residues in the Rab family are highlighted in gray. The P-loop and switch regions are labeled and indicated by black lines. The pink lines mark the four Rab subfamily–specific sequence regions (RabSF1–4). The SidM-binding residues in Rab1 are denoted by red asterisks on top of the sequence. The SidM-binding residues in Rab1 that are solvent-exposed in the Ypt1-GDI complex are indicated by blue squares underneath the sequence.

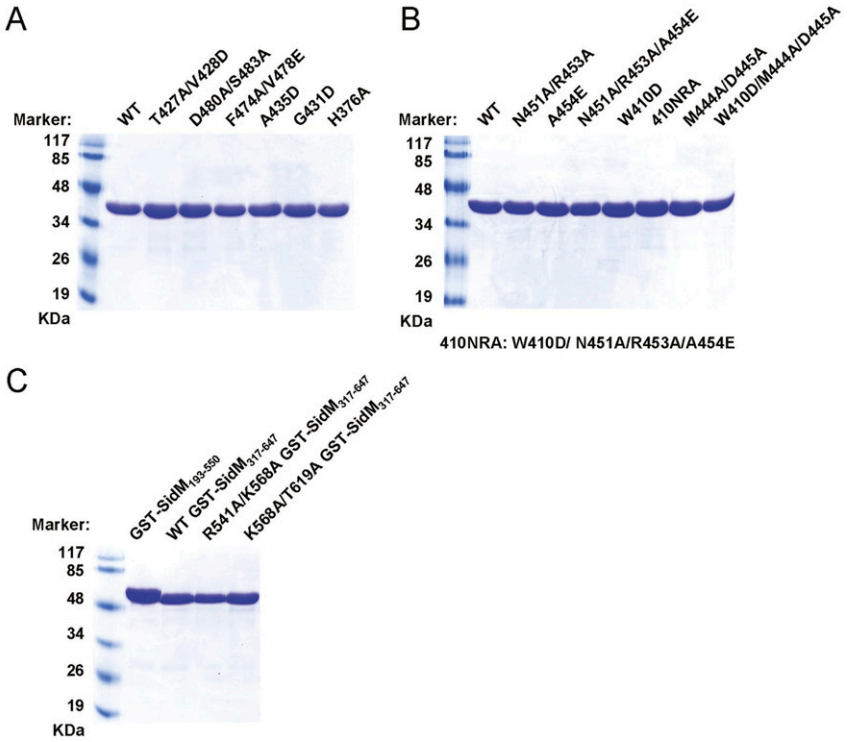

Fig. S5. SDS/PAGE and Coomassie blue staining of mutant SidM proteins used in this study. (*A*) WT and mutant $SidM_{193–550}$ proteins used in Fig. 3 *C* and *D*. (*B*) WT and mutant $SidM_{193–550}$ proteins used in Fig. 3 *E* and *F*. (*C*) GST fusion proteins used in Fig. 2*C*.

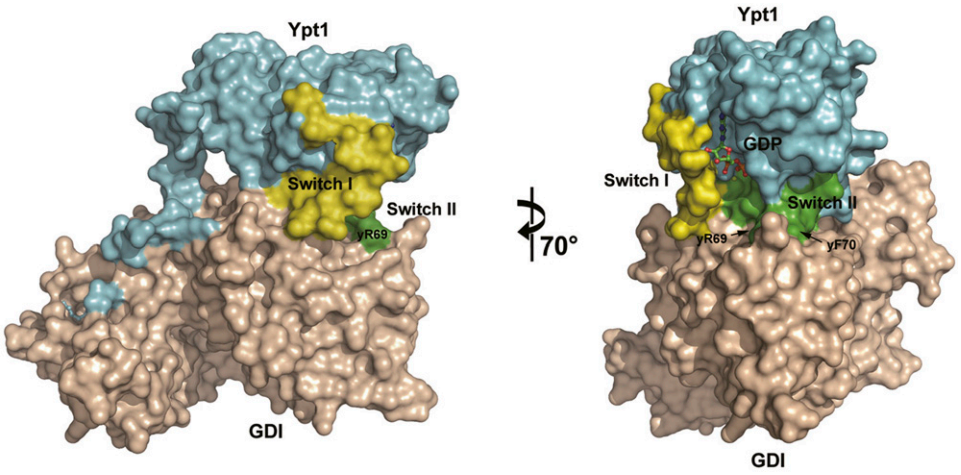

Fig. S6. The solvent-exposed surface of Ypt1 in the Ypt1-GDI complex. The Ypt1-GDI complex is presented as surface with Ypt1 in cyan and GDI in gray. The switch I (yellow) and switch II (green) regions are highlighted. GDP and magnesium bound in Ypt1 (green) are represented as ball-and-stick and sphere, respectively. The partially exposed residues yR69 and yF70 in switch II of Ypt1 are indicated.

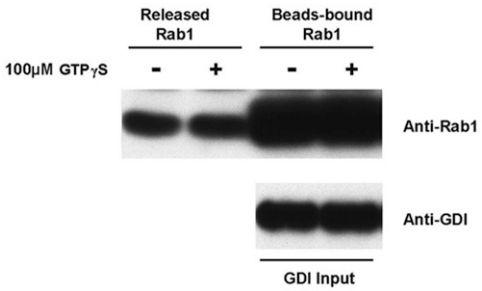

Fig. S7. Effects of 100 μM of GTPγS on SidM-catalyzed GDI displacement. The GDI displacement assay was performed as shown in Fig. 5*F*, except that 100 μM of GTPγS was included in the reaction. Released Rab1 resulting from SidM activity and bead-bound Rab1 were detected by anti-Rab1 Western blot analysis, and the amounts of GDI used in each reaction are shown in the lower panel as anti-GDI Western blot.

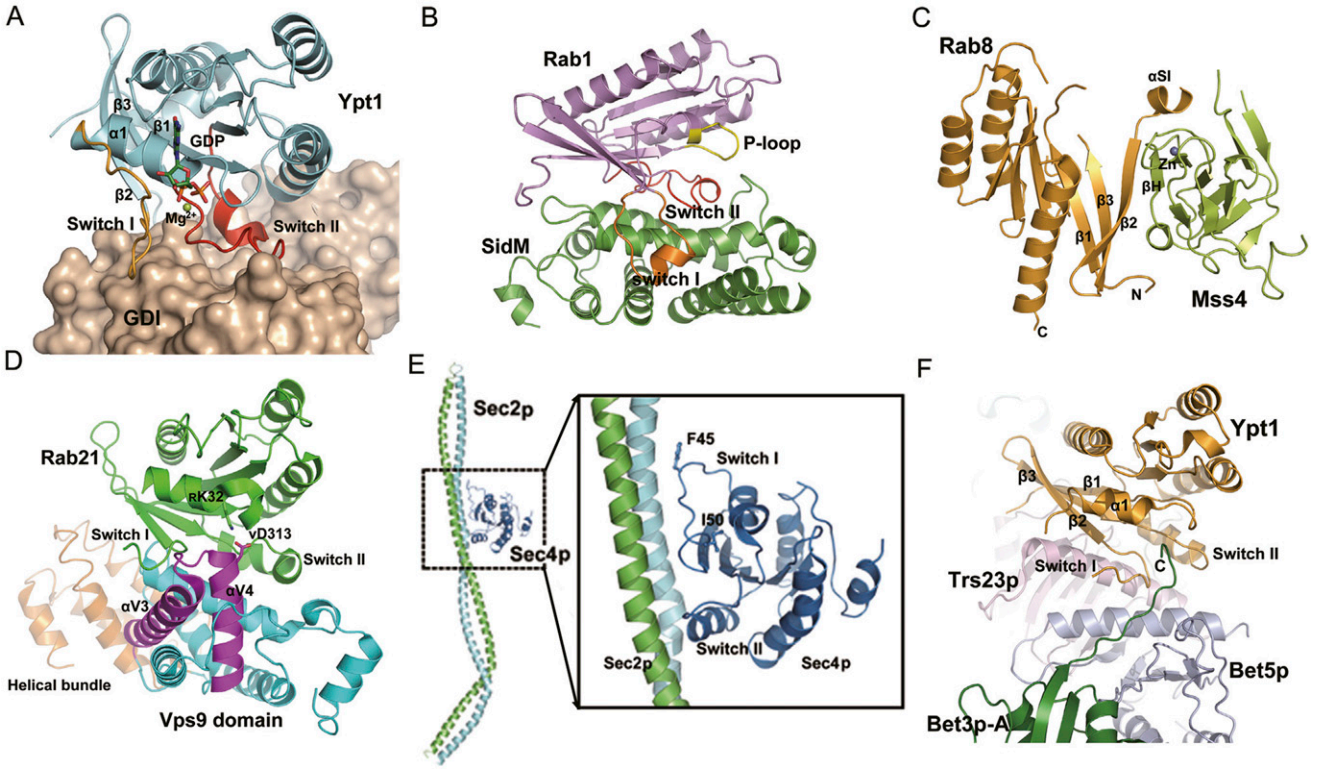

Fig. S8. Structural comparisons of the SidM-Rab1 complex with various RabGEF-Rab complexes. (*A*) Structure of the Ypt1-GDI complex, with Ypt1 in sticks (cyan) and GDI in surface presentation (gray). Switch I and switch II are in orange and red, respectively. (*B*) Complex structure of Rab1 and the SidM Rab1-activation domain. Rab1 and SidM are color-coded as in Fig. 1*B*. Switch regions and the P-loop of Rab1 are indicated. (*C*) Structure of the Mss4-Rab8 complex (PDB ID code 2FU5). Rab8 is in yellow, and Mss4 is in green. The Mss4-binding region in Rab8 and β_H in Mss4 that forms the intermolecular β-sheet with Rab8 are indicated. Zinc ion bound in Mss4 is shown as a gray ball. (*D*) Structure of Rab21 in complex with the tandem helical bundle and VPS9 domain of Rabex5 (PDB ID code 2OT3). Rab21 is in green. The helical bundle and the VPS9 domain are in orange and cyan, respectively, with the two helices wedged into the space between the indicated switch I and II of Rab21 highlighted in purple. K32 in the P-loop of Rab21 and the aspartic-finger residue D313 of the VPS9 domain are shown as ball-and-stick representations. (*E*) Structure of the Sec2p-Sec4p complex (PDB ID code 2OCY). The dimeric coil-coil structure of Sec2p is in green and cyan. Sec4p is in blue. The displaced F45 and I50 of Sec4p critical for the release of magnesium are shown as ball-and-stick representations. Switch regions of Sec4p are also indicated. (*F*) Structure of the multimeric TRAPP I complex bound with Ypt1 (PDB ID code 3CUE). Three subunits (Bet3p-A, Bet5p, and Trs23p) of the TRAPP I complex that interact with Ypt1 are shown in green, light gray, and light red, respectively. Ypt1 is in orange. The TRAPP I complex binds to β1, interswitch, the C terminus of switch I, and the whole switch II regions of Ypt1. The C terminus of Bet3p wedged into the nucleotide-binding pocket is marked with a "C".

Table S1. Data collection and refinement statistics

	$SidM_{317–647}$	$SidM_{193–550}$–$Rab1_{177}$ complex
Data collection		
Space group	$P4_1$	$P2_1$
Cell dimensions		
A, b, c, Å	144.337, 144.337,102.280	63.808, 71.747, 146.911
α, β, γ, °	90.00, 90.00, 90.00	90.000, 93.623, 90.000
	Se-Peak	Se-Peak
Wavelength	0.97917	0.97912
Resolution, Å	20–3.45 (3.57–3.45)	50–2.85 (2.90–2.85)
R_{merge}	10.3 (95.4)	10.3 (54.2)
I/σ(I)	26.5 (3.6)	25.6 (5.1)
Completeness, %	98.9 (100.0)	99.6 (99.3)
Redundancy	8.9 (9.1)	7.5 (7.5)
Refinement		
Number of reflections	27,365	27,782
R_{work}/R_{free}	21.45/24.05	22.56/26.58
Number of atoms		
Protein	5,101	7,658
Ligand/ion	10	22
Water		24
RMS deviations		
Bond lengths, Å	0.007	0.007
Bond angles, °	1.30	1.04

Data for the highest-resolution shell are given in parentheses.